CLM - P 575

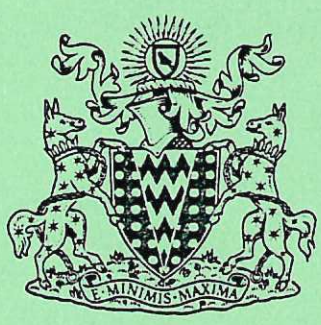

UKAEA

Preprint

SHEAR DAMPING OF TWO-DIMENSIONAL DRIFT WAVES IN A LARGE ASPECT RATIO TOKAMAK

R J HASTIE
K W HESKETH
J B TAYLOR

CULHAM LABORATORY
Abingdon Oxfordshire

1979

CLM-P 575

SHEAR DAMPING OF TWO-DIMENSIONAL DRIFT WAVES IN A LARGE ASPECT RATIO TOKAMAK

R.J. Hastie, K.W. Hesketh, J.B. Taylor

Culham Laboratory, Abingdon, Oxon., OX14 3DB, UK

(Euratom/UKAEA Fusion Association)

ABSTRACT In a uniform plane slab, with shear in the magnetic field, damping of drift waves is due to the outward convection of energy by the wave. It is known, however, that the inclusion of two-dimensional effects, such as toroidal modulation of shear or magnetic field, can inhibit propagation of the wave and so reduce shear damping. This effect is investigated using a two-dimensional model representing long wavelength drift waves in a large aspect ratio Tokamak. It is shown that this two-dimensional problem can be reduced to a one-dimensional eigenvalue equation from which the shear damping can readily be computed. It is confirmed that toroidal effects can annul the shear damping and some examples are given.

(Submitted for publication in Nuclear Fusion)

February 1979

1. INTRODUCTION

The damping of drift waves in a sheared magnetic field has been intensively studied using the plane slab model [1,2,3] in which the shear and magnetic field strength are uniform. This "shear-damping" can be attributed to the fact that in the presence of shear, drift waves convect energy away from the central rational surface (at which $k_{\parallel} = 0$). However, in a toroidal system the magnitude, the shear and the curvature of the magnetic field are no longer uniform over a magnetic surface and Taylor [4] has pointed out that this non-uniformity induces a coupling between modes centred on different rational surfaces which can inhibit convection of energy and so reduce the shear damping.

The calculations of Ref. [4] were based on a very idealised model and were restricted to the limits of weak and strong modulation. A more accurate model, appropriate to long wavelength drift waves in a large aspect ratio tokamak, has been studied by Cordey and Hastie [5]. However, due to difficulties associated with periodicity in the poloidal variable, they investigated only modes which are highly localised in this direction - a restriction equivalent to the strong modulation limit of Ref. [4].

In the present work we re-examine shear damping of drift waves in a toroidal system, and carry out numerical computations of the transition from weak to strong coupling using the more accurate model of Ref. [5]. The periodicity difficulty is dealt with by the method described by Connor, Hastie and Taylor [6].

2. THE PERIODICITY PROBLEM

In any axisymmetric system the calculation of linear drift wave eigenmodes can be reduced (after Fourier decomposition $\sim \exp i N\zeta$, in the ignorable co-ordinate ζ) to a two-dimensional eigenvalue problem of the form [6, 7]

$$\mathcal{L}(\theta,x;\omega)\ \phi(\theta,x) = 0 \tag{1}$$

In general $\mathcal{L}$ is an integral operator in the periodic poloidal variable θ and the flux surface co-ordinate x. However, it reduces to a differential operator in both variables in certain limiting cases.

Since drift waves are characterised by short perpendicular and long parallel wavelengths a natural representation for the perturbed quantities would be in an eikonal form

$$\phi(\theta,x) = F(\theta,x)\ \exp\ (iNS(\theta,x)) \tag{2}$$

with the toroidal mode number $N \gg 1$ and both $F(\theta,x)$ and $S(\theta,x)$ varying on the equilibrium scale. The long parallel wavelength requires $\underset{\sim}{B}\cdot\nabla(\zeta + S) = 0$, but such a representation violates the periodicity constraint in the poloidal angle θ. We therefore follow the procedure of Connor et al. [6] and introduce the transformation

$$\phi(\theta,x) = \sum_m e^{-im\theta} \int_{-\infty}^{\infty} e^{im\eta}\ \hat{\phi}(\eta,x)\ . \tag{3}$$

This takes the problem from the periodic domain $0 \leq \theta < 2\pi$ into the infinite domain $-\infty < \eta < +\infty$, leaving the operator $\mathcal{L}$ and the eigenvalue ω unchanged, and allows us to use the eikonal representation (2) for $\hat{\phi}(\eta,x)$ (which need not be periodic in η). Then

in the limit of large N, as in the similar problem of MHD ballooning modes [6, 7], the two-dimensional eigenvalue problem reduces to two separate one-dimensional equations in η and in x respectively.

3. MODEL EQUATION FOR DRIFT WAVES IN A TOKAMAK

In the following we adopt the two-dimensional eigenmode equation derived in Ref. [5], which describes long wavelength ($k_\perp a_i \ll 1$) drift waves in a large aspect ratio ($\varepsilon = a/R \ll 1$) tokamak of circular cross-section with $\beta \sim \varepsilon^2$. Dissipative effects such as electron and ion landau damping or collisions are neglected so that the only contribution to $\mathrm{Im}\,\omega$ arises from shear induced damping. Our objective is to determine the effect of toroidal coupling on this shear damping and, in particular, to compare damping in this toroidal model with that in a plane slab with similar shear.

The perturbation may be written in the form

$$\phi(\theta, x) \exp\left[i(N\zeta - M\theta - \omega t) \right]$$

where the radial, flux surface, coordinate r has been replaced by a local coordinate $x = (r - r_o)$ with $Nq(r_o) = M$ (integer), $q = r B_\zeta / R B_\theta$. Then, with the poloidal angle measured from the outside of the torus, the appropriate eigenvalue equation for long wavelength drift waves can be written:

$$a_i^2 \frac{\partial^2 \phi}{\partial x^2} - k^2 a_i^2 \phi - \left(\frac{\omega_*}{\omega} \frac{\varepsilon_c}{k a_i}\right)^2 \left(\frac{\partial}{\partial \theta} + iksx\right)^2 \phi + \frac{(\omega_* - \omega)}{(\omega_* + \omega\tau)} \phi$$

$$- 2 \frac{\omega_*}{\omega} \varepsilon_n \left(\cos\theta + \sin\theta \frac{i}{k} \frac{\partial}{\partial x}\right)\phi = 0 \qquad (4)$$

where $s = (r/q)(dq/dr)$, $\tau = T_e/T_i$, $k = Nq/r$, $\varepsilon_n = q\,\varepsilon_c = r_n/R\tau$,

$a_i^2 = T_i/M_i\omega_{ci}^2$ and $\omega_* = k T_e/e B r_n$ with $r_n^{-1} = n^{-1}(dn/dr)$.

In Eq. (4) the trapped electron contribution to the charge density has been dropped so that the dominant modulation term arises from the ion magnetic drift, with both the principal curvature ($\sim \cos\theta$) and the geodesic curvature ($\sim \sin\theta$) appearing. In other respects Eq. (4) has the same form as in slab geometry. [Effects such as landau-damping, trapped particles etc. can be incorporated in the formalism if the transformation (3) is applied to the basic Vlasov equations rather than to the charge neutrality equation.]

Eq. (4) is of the general type discussed in the preceding section so we write

$$\phi(\theta,x) = \sum_m e^{-im\theta} \int_{-\infty}^{\infty} e^{im\eta}\, \hat{\phi}(\eta,x)\, d\eta \tag{5}$$

and

$$\begin{aligned} \hat{\phi} &= F(\eta, x)\, \exp\left[\, i(M - Nq)(\eta - \eta_o)\,\right] \\ &= F(\eta, x)\, \exp\left[\, - iksx(\eta - \eta_o)\,\right] \end{aligned} \tag{6}$$

where η_o is an arbitrary phase of the eikonal. Introducing (5) and (6) into Eq. (4) we obtain the following equation for $F(\eta,x)$,

$$\begin{aligned} &- k^2 a_i^2 \left(s\eta + \frac{i}{k}\frac{\partial}{\partial x}\right)^2 F - \left(\frac{\omega_* \varepsilon_c}{\omega\, k a_i}\right)^2 \frac{\partial^2 F}{\partial \eta^2} + \left(\frac{\omega_* - \omega}{\omega_* + \omega\tau} - k^2 a_i^2\right) F \\ &\quad - 2\,\frac{\omega_*}{\omega}\,\varepsilon_n \left(\cos(\eta + \eta_o) + s\eta \sin(\eta + \eta_o) + \sin(\eta + \eta_o)\cdot \frac{i}{k}\frac{\partial}{\partial x}\right) F = 0 \end{aligned} \tag{7}$$

The strong x-dependence of the perturbation (i.e. on the scale of the perpendicular wavelength) associated with the shear has now been removed, but F still depends weakly on x since the parameters in Eq.(7), such as ω_*, themselves vary slowly (i.e. on the equilibrium scale) with radius.

[This variation is most important in the term $(\omega_* - \omega)/(\omega_* + \omega\tau)$; elsewhere it appears with a small factor ka_i, ε_c or ε_n.]

Eq.7 is our basic model for long wavelength drift waves in a large aspect ratio torus. As described in the Appendix, an expansion in the ratio of the perpendicular wavelength of the perturbation to the equilibrium scale length, represented formally by the small parameter $h = k^{-1}(\partial/\partial x)$, reduces the problem to an ordered set of equations. The zero-order approximation is clearly an ordinary differential equation in the extended poloidal variable alone. This lowest order equation takes the form

$$\frac{d^2F_o}{d\eta^2} + [\lambda - U(\eta)]\, F_o(\eta) = 0 \qquad (8)$$

with

$$U(\eta) = -\sigma^2[\eta^2 + 2\alpha(\cos(\eta + \eta_o) + s\eta \sin(\eta + \eta_o))] \qquad (9)$$

where

$$\sigma \equiv \frac{\omega}{\omega_*}\frac{k^2a_i^2s}{\varepsilon_c} \quad , \quad \alpha = \frac{\varepsilon_n}{k^2a_i^2s^2}\left(\frac{\omega_*}{\omega}\right)$$

and

$$\lambda = \left(\frac{\omega}{\omega_*}\frac{ka_i}{\varepsilon_c}\right)^2\left(k^2a_i^2 - \frac{\omega_* - \omega}{\omega_* + \omega\tau}\right) \quad .$$

The eigenvalue $\omega = \omega_o$ obtained from Eq.(8) depends on the parameter η_o and also varies slowly with radius. Nevertheless it represents the leading approximation (in powers of h) to the eigenvalue ω of the basic, two dimensional, Eq.(7).

The relationship of this local eigenvalue ω_o to the true eigenvalue ω is determined by the higher order theory described in the Appendix.

The parameter η_o can be regarded as specifying the centre of the perturbation and we can therefore anticipate the result of the higher order theory - that in configurations with symmetry about $\theta = 0$ this centering parameter will take the value 0 or π. [In computations this is equivalent to permitting the parameter α to take either sign: positive values correspond to $\eta_o = 0$ and to modes centred on the outside of the torus, negative values correspond to $\eta_o = \pi$ and to modes centred on the inside.]

Eq.(8) has the form of a Schrödinger equation with an effective potential $U(\eta)$, but this potential is itself a function of ω which may be complex. In the absence of toroidal curvature ($\alpha = 0$) and for real ω, this potential $U(\eta)$ is a parabolic "anti-well". In this case the eigenfunctions will be propagating waves in η-space which transform into the shear-damped, outgoing wave, solutions of the conventional plane slab model. This brings out one advantage of the present formalism, - that it makes it particularly easy to visualise the effect of toroidal curvature on shear damping. The curvature introduces modulations into the effective potential $U(\eta)$ which modify and inhibit wave propagation. If the modulation is sufficiently strong it leads to the formation of local potential wells and so to non-propagating, undamped modes - analogous to bound states of the Schrödinger equation. In particular, a local minimum of $U(\eta)$ may occur at the origin when $\alpha(1 - 2s) > 1$ for $\eta_o = 0$ and when $\alpha(2s - 1) > 1$ for $\eta_o = \pi$. Other local minima, at $\eta > 1$, may occur when $\alpha s > 1$ for $\eta_o = 0$ or π.

The potential function $U(\eta)$ for $s = 1$ is shown in Fig.1 for $\eta_o = 0$ and in Fig.2 for $\eta_o = \pi$. Local minima do indeed arise when $\alpha > 1$ but a noteworthy feature is the extremely shallow nature of these central wells. A much more effective "double-well" can appear when the origin is a local maximum (Fig.2). This suggests that strong coupling

theory [5,8], which is equivalent to an expansion of $U(\eta)$ around $\eta = 0$, may sometimes be misleading since it does not recover the off-centre minima. In Section 7 we shall therefore compare the damping predicted by such a local expansion with that obtained by a numerical solution of Eq.(8).

4. BOUNDARY CONDITIONS

In real space the boundary conditions are that $\phi(\theta,x)$ should vanish as $|x| \to \infty$, or that it should represent outgoing waves. The former corresponds to localised modes and the latter to propagating shear damped, modes [1] with outward energy flux. We must first interpret what this "outgoing energy flux" condition implies for the boundary condition on Eq.(8) at $|\eta| \to \infty$. The simplest way to do this is to consider an unstable mode. Then an outgoing wave will decay as $|x| \to \infty$. Hence, for $\text{Im}\ \omega > 0$ the mode must be bounded in x-space and consequently $F(\eta)$ must be such that the transformation (3) converges as $|\eta| \to \infty$. Now as $|\eta| \to \infty$ the two solutions of Eq.(8) are $F_+ \sim \exp(i\sigma\eta^2/2)$ and $F_- \sim \exp(-i\sigma\eta^2/2)$ and, since $\text{Im}\ \sigma > 0$ when $\text{Im}\ \omega > o$, only F_+ is convergent and acceptable. Consequently the boundary condition on Eq.(8) in the η domain must be that $F \to F_+$ as $|\eta| \to \infty$.

A similar conclusion can be drawn by introducing damping into the model at large $|x|$ to ensure that all modes decay in real space. Then the transformation (3) must again converge and requires $F \to F_+$ $|\eta| \to \infty$.

Because Eq.(8) is symmetric in η we need consider only symmetric and antisymmetric modes, with boundary conditions

$$\left.\frac{dF}{d\eta}\right|_o = 0 \text{ (even mode)} \quad , \quad \text{or} \quad F(o) = 0 \text{ (odd mode)}$$

and $F(\eta) \to F_+(\eta)$ as $\eta \to +\infty$. Most of the calculations of Section (7) refer to even modes, which suffer the least damping.

5. THE PROBLEM OF ASYMPTOTIC MATCHING

The problem as posed above is not readily amenable to numerical solution. When the modes are stable ($\mathrm{Im}\ \omega < 0$) the asymptotic solution F_+ is increasing exponentially with η, while F_- is decreasing exponentially. The eigenvalue condition is that the solution F_- be rejected in the asymptotic matching but, since F_- is in any event exponentially small in the matching region, this condition cannot be determined accurately.

This difficulty can be avoided by introducing an artificial destabilising term and studying only marginally stable modes. These are purely oscillatory as $\eta \to \infty$ and the difficulty of matching onto exponentiating solutions does not arise.

We therefore add to the electron charge density a simple destabilising term of the form $-i\phi\delta$, with δ a real constant. The mode equation then becomes

$$\frac{d^2F}{d\eta^2} + [\lambda - i\hat{\delta} - U(\eta)]F = 0 \qquad (10)$$

with λ and U as defined in Section (2) and

$$\hat{\delta} = \left(\frac{\omega}{\omega_*}\,\frac{ka_i}{\varepsilon_c}\right)^2 \frac{\omega\delta}{(\omega_* + \omega\tau)} \ .$$

Equation (10) is solved numerically for real ω and real δ and the eigenvalue δ_m then represents the shear damping as measured by the magnitude of the electron destabilising term needed to produce marginally stable drift waves. It is this quantity which is henceforth referred to as "shear damping".

6. NUMERICAL METHOD

Eq. (10) has been solved by a numerical shooting method, using a sixth order Numerov scheme [9]. With ω real the asymptotic solution F_+ is constructed at the end of the mesh. Using this asymptotic solution as starting value the function $F(\eta)$ is then computed, by shooting inwards, and tested against the required boundary condition $(dF/d\eta)_o = 0$. The values of ω and δ are iterated until this condition is satisfied. Typically the asymptotic matching is carried out at $\eta \sim 10\text{-}12$ and ω and δ are obtained to an accuracy better than $\frac{1}{2}\%$ using around 30 steps per period in η.

7. RESULTS

At this point, before we discuss the numerical results, it is useful to summarise the steps involved in the analysis. We have taken a two-dimensional model equation representing long wavelength drift waves, which incorporates non-uniform ion drifts in the toroidal field and we have transformed the calculation from the periodic poloidal domain θ into the infinite domain η to overcome the periodicity difficulty so that we may exploit the eikonal approximation. Then in lowest order in the small parameter h the complex frequency ω is determined by the ordinary differential Eq. (8) in the extended poloidal variable η. However, for practical convenience we have chosen instead to make ω real by introducing a destabilising term δ, whose value is then a measure of the effective shear damping.

This effective shear damping δ_m has been computed from Eq. (10) as a function of the model parameters $s, ka_i, \tau, \varepsilon_c, \varepsilon_n$. (We recall that s represents the shear, k represents the effective wavenumber of the mode, τ is the ratio of electron and ion temperatures,

and the parameters $\varepsilon_c = r_n/R\, q\tau$ and $\varepsilon_n = r_n/R\, \tau$ are measures of the connection length and field line curvature respectively.) In the first set of calculations the parameters s, ka_i, ε_c and τ were held constant as the parameter ε_n was varied. This gives a direct indication of the effect of the toroidal modulation on the damping of drift waves. In the second set of calculations ka_i was fixed and the other parameters varied in a manner which simulates a radial traverse through the minor cross-section of the DITE tokamak.

(i) $s, ka_i, \varepsilon_c, \tau$ constant and ε_n varying

The values taken for the fixed parameters were: $s = 1.0$, $k^2a_i^2 = 0.1$, $\varepsilon_c = 0.1$ and $\tau = 1.0$. (The choice of ka_i is arbitrary, the other parameters represent typical tokamak values.) In Fig. 3 we show δ_m as a function of ε_n, normalised to the plane slab ($\varepsilon_n = 0$) value, which for our model is $\varepsilon_c s (1 + \tau)(1 + b\tau)/(1 - b)^2$.

For $\eta_o = 0$ the damping at first increases with increasing ε_n. This corresponds to the increasing curvature of the central "anti-well" at $\eta = 0$ (see Fig. 1a, 1b) which increases the outward wave propagation. Then at a value of $\varepsilon_n \simeq 0.05$ an off-centre local minimum forms in the effective potential $U(\eta)$ (see Fig. 1c, 1d). At this point the least damped mode becomes localised around this minimum (in Schrödinger equation terms a partially bound state is created). As ε_n is increased further this mode becomes more tightly bound, the propagated wave becomes smaller and the damping falls rapidly to near zero.

For $\eta_o = \pi$ the damping δ_m decreases continuously as ε_n is increased. At small ε_n this decrease is due to a flattening of the central anti-well (see Fig. 2a, 2b) which reduces outward wave

propagation. Beyond $\varepsilon_n \simeq 0.13$ a central local minimum forms (see Fig. 2d) where a partially bound state is again created. However as this minimum is very shallow, and the damping already small, the effect of this on δ_m is less abrupt than for modes with $\eta_o = 0$.

The dependence of ω/ω_* on ε_n is shown in Fig.4. For $\eta_o = 0$ the mode is centred on the outside of the torus where it experiences unfavourable curvature leading to a decrease in ω/ω_*. For $\eta_o = \pi$ the mode is centred on the inside of the torus where the favourable curvature causes an increase in ω/ω_* which can rise above unity. [In practice this may be an important stabilising mechanism since the true electron Landau resonance may then stabilise rather than destabilise the mode.]

Dependent on the height and width of the "potential barrier" responsible for localising the mode, there may exist additional solutions of the eigenvalue equation, corresponding to excited bound states of the Schrödinger equation. One such "excited state" has been found for $\eta_o = 0$, and the dotted curves in Figs.3 and 4 show δ_m and ω/ω_* for this mode.

From these calculations we see that the most dangerous modes, in the sense of having the least shear-damping, may be those associated with minima of $U(\eta)$ which occur elsewhere than at the origin and calculations [5,8] which are equivalent to expanding $U(\eta)$ around the origin may therefor sometimes give misleading results. To investigate this we replace $U(\eta)$ by an expansion around $\eta = 0$;

$$U(\eta) = \sigma^2\{\mp 2\alpha - [1 \pm \alpha(2s - 1)]\eta^2\} \qquad (11)$$

where the upper sign refers to $\eta_o = 0$ and the lower to $\eta_o = \pi$. Then Eq.(10) can be solved analytically to give:

$$\left(\frac{\omega}{\omega_*}\right)^2 [1 + k^2 a_i^2 \tau] - \frac{\omega}{\omega_*} [1 - k^2 a_i^2 \mp 2\varepsilon_n \tau] \pm 2\varepsilon_n = 0 \qquad (12)$$

$$\delta_m = \varepsilon_c s \frac{\omega_* (\omega_* + \omega\tau)}{\omega^2} \left[1 \pm \frac{\varepsilon_n}{k^2 a_i^2 s^2} \frac{\omega_*}{\omega} (2s - 1)\right]^{\frac{1}{2}} \qquad (13)$$

This approximation for δ_m is shown in Fig.5 and it will be seen that although it gives good agreement with the numerical results for $\varepsilon_n \lesssim 0.05$ the analytic expression fails for larger ε_n when off-centre minima in $U(\eta)$ become important.

(ii) Radial Traverse through a Tokamak

To investigate whether the reduction of shear damping by toroidal effects is likely to be significant in practical devices we have considered a typical discharge in the DITE experiment [10] which has an aspect ratio $\sim 1/5$. At 200 kA the safety factor and the density are represented by $q(r) = 1 + 4(r/a)^2$ and $n = 1 - (r/a)$ respectively. Using these expressions we have computed the local shear damping δ_m as a function of radius (taking $T_e = T_i$ and $(ka_i)^2 = 0.1$ uniform across the radius). Comparison of this computed value of δ_m with the plane slab model for the same local parameters is shown in Fig.6. It is clear that there are two distinct regions:

(i) an inner core region within which the shear damping is almost completely annulled by the toroidal modulations. This region extends out to $r/a \lesssim 0.25$ for modes centred on the inside of minor cross section, and out to $r/a \lesssim 0.5$ for modes centred on the outside.

(ii) an outer region in which the shear damping approaches its plane slab value as $r/a \to 1$, but within which it may be enhanced (for modes on the outside) or reduced (for modes on the inside) by as much as a factor 3 at intermediate values of r/a.

These results can be understood in terms of the potential $U(\eta)$. Consider first the case $\eta_o = \pi$. For $r/a < 0.25$ the shear parameter $s < \frac{1}{2}$ so that a central minimum cannot form. However the toroidal modulation is strong in this region so that off-centre minima occur as in Fig. 7a. The undamped modes for $\eta_o = \pi$ and $r/a \lesssim 0.25$ correspond to bound states in or between these off-centre minima. For $r/a \gtrsim 0.3$ the shear parameter exceeds $\frac{1}{2}$ so that central minima in $U(\eta)$ might be expected, but in this region the toroidal modulation is too weak for this to occur so that there is only a partial flattening of the central "antiwell" (Fig. 7b).

When $\eta_o = 0$ a central minimum does occur for $r/a < 0.3$ (where $s < \frac{1}{2}$ and toroidal modulation is strong) and the undamped modes for $\eta_o = 0$ and $r/a \lesssim 0.3$ correspond to bound states in such a central minimum (Fig.7c). However, in the region $0.3 < r/a < 0.5$ (where $s > \frac{1}{2}$) the centre is again a local maximum and the continuation of the undamped modes into this region is due to the off-centre minima as in Fig. 7d. Beyond $r/a \sim 0.5$ toroidal effects again become too weak to maintain the double well structure and the predominant effect is the increase of the antiwell curvature around $\eta = 0$ (Fig. 7e) leading to increased damping. As $r/a \to 1$ this effect decreases as the toroidal effects themselves become weaker.

We see from this example that in a practical system the toroidal effects are indeed important and can almost completely annul the shear damping. We also see that this annulment can arise in more than one way.

8. CONCLUSIONS

It was suggested in Ref.[4] that the shear damping of drift waves in a toroidal system can be quite different to that in the conventional plane slab model (in which the field and shear are uniform) with similar

average parameters. In the slab, shear damping is due to the convection of energy from the central mode rational surface; in a toroidal system modes centred on different rational surfaces are coupled so that energy convection is inhibited.

In the present paper we have investigated this in a more realistic model (derived from that of Ref.[5]) which represents a large aspect ratio, circular cross section, toroidal system. After a transformation of the poloidal coordinate to the infinite domain the problem of shear damping is again represented as one of wave propagation - but now in a varying effective potential $U(\eta)$ whose characteristics depend on the degree of toroidal modulation of the field.

This investigation confirms that toroidal effects can indeed annul the shear damping of drift waves. However it also shows that this can occur in more complicated ways than originally envisaged. Not only can the wave energy be trapped in a central minimum of $U(\eta)$, it can also be trapped in off-centre minima of $U(\eta)$. Indeed these off-centre minima can occur when the toroidal effect is too small to create a central minimum. Consequently approximations [5,8] which are equivalent to an expansion of the potential $U(\eta)$ around $\eta = 0$ may sometimes be misleading.

Although our model still represents a considerable idealisation of a real confinement system, an application of our calculations to the parameters of a typical Tokamak, such as DITE, suggests that in practice toroidal effects are indeed large enough to substantially affect shear damping.

ACKNOWLEDGEMENT

The authors are grateful to J.W. Connor for many helpful discussions on this work.

APPENDIX

HIGHER ORDER THEORIES

In the main text we have investigated the difference between shear damping of drift waves in a toroidal system and in the conventional plane slab. For this the lowest order approximation in the ratio of perturbation wavelength to equilibrium scale length is sufficient. It involves only an ordinary differential equation, in the extended poloidal variable η, whose eigenvalue $\omega_o(\eta_o)$ is an approximation to the true eigenvalue ω. However to demonstrate the formal connection between ω_o and ω, to determine η_o and to find the full structure of the perturbation a higher order theory would be required. The development of this, which resembles that for the corresponding MHD problem [7,11], is described below.

In the present model the underlying, two-dimensional equation for drift waves is Eq.4. After transformation of the poloidal variable to the infinite domain η and introduction of the eikonal representation this becomes Eq.(7) of Section 3 which we can take as the starting point for development of higher order approximations. It is convenient to re-write this as

$$k^2a_i^2\left(s(\eta - \eta_o) - \frac{ih}{k}\frac{\partial}{\partial x}\right)^2 F + \left(\frac{\omega_* \varepsilon_n}{\omega\, ka_i}\right)^2 \frac{\partial^2 F}{\partial \eta^2} - \left(\frac{\omega_* - \omega}{\omega_* + \omega\tau} - k^2a_i^2\right)F$$

$$+ \frac{2\omega_* \varepsilon_n}{\omega}\left(\cos\eta + s(\eta - \eta_o)\sin\eta + \sin\eta \cdot \frac{ih}{k}\frac{\partial}{\partial x}\right)F = 0 \qquad (A.1)$$

We now seek solutions of this equation which vary slowly compared to the short wavelength k^{-1}. To facilitate this we have introduced in (A.1) a formal ordering parameter h (finally to be set equal to unity) which identifies the order of magnitude of each term in an expansion in $(k^{-1}(\partial/\partial x)$. In this expansion we take $\varepsilon_n \sim \varepsilon_c \sim (\omega_* - \omega)/\omega \sim k^2a_i^2$.

The leading approximation of any expansion in h will be

$$\mathcal{L}_o F_o = 0 \tag{A.2}$$

where $\mathcal{L}_o(\eta, \eta_o, \omega_o, x)$ is :

$$\mathcal{L}_o = (k a_i s)^2 (\eta - \eta_o)^2 - \left(\frac{\omega_* - \omega_o}{\omega_* + \omega\tau} - k^2 a_i^2\right) + \left(\frac{\omega_*}{\omega} \frac{\varepsilon_c}{k a_i}\right)^2 \frac{\partial^2}{\partial \eta^2}$$

$$+ 2 \frac{\varepsilon_n \omega_*}{\omega} (\cos\eta + s(\eta - \eta_o) \sin\eta) \tag{A.3}$$

Equation A.2 is that studied in the main text; it leads to an eigenvalue $\omega_o(\eta_o, x)$ and an eigenfunction $f_o(\eta, x)$. However since (A.2) is an ordinary differential equation in η alone, f_o may be multiplied by an arbitrary function $A(x)$, making the full solution

$$F_o = A(x)\ f_o(\eta, x)\ . \tag{A.4}$$

We now assume that this "amplitude" $A(x)$ varies on some scale intermediate between the equilibrium scale length and the wavelength k^{-1}. This is represented formally by writing $A = A(y)$ where y is a scaled variable, $x = h^{1-\nu} y$. We then develop F in ascending powers of h. If $0 < \nu \leq \frac{1}{2}$ the first terms in such a development are

$$F = A(y)\ f_o(\eta, x) + h^{\nu} F_1(\eta, y, x) + h^{2\nu} F_2(\eta, y, x) \tag{A.5}$$

and the functions F_1 and F_2 satisfy

$$\mathcal{L}_1 f_o A + \mathcal{L}_o F_1 = 0 \tag{A.6}$$

and

$$\mathcal{L}_2 (f_o A) + \mathcal{L}_1 F_1 + \mathcal{L}_o F_2 + \frac{\partial \mathcal{L}_o}{\partial \omega_o} \{\omega - \omega_o(x)\} = 0 \tag{A.7}$$

In this last equation we have treated the difference between the true (ω) and local ($\omega_o(x)$) eigenvalues as of order $h^{2\nu}$; we shall return to this point later. The operators $\mathcal{L}_1$ and $\mathcal{L}_2$ are defined by

$$\mathcal{L}_1 = -\frac{i}{ks}\frac{\partial \mathcal{L}_o}{\partial \eta_o}\cdot\frac{\partial}{\partial y} \tag{A.8}$$

$$\mathcal{L}_2 = -\frac{1}{2(ks)^2}\frac{\partial^2 \mathcal{L}_o}{\partial \eta_o^2}\cdot\frac{\partial^2}{\partial y^2} \quad . \tag{A.9}$$

The operator $\mathcal{L}_o$ is self adjoint for functions $f_o(\eta)$ which $\to 0$ as $|\eta| \to \infty$ and the integrability condition on (A.6) is therefore

$$\int f_o(\eta, x)\frac{\partial \mathcal{L}_o}{\partial \eta_o} f_o(\eta, x)\, d\eta \equiv \left\langle f_o \frac{\partial \mathcal{L}_o}{\partial \eta_o} f_o \right\rangle = 0 \tag{A.10}$$

Recalling that $\langle f_o \mathcal{L}_o f_o \rangle = 0$ for all η_o, this is equivalent to

$$\frac{\partial \omega_o}{\partial \eta_o} = 0 \tag{A.11}$$

which determines the hitherto unknown phase η_o. In our model symmetry ensures that (A.11) is satisfied when $\eta_o = 0$ or $\eta_o = \pi$. Then Eq. (A.6) is easily solved for F_1;

$$F_1 = -\frac{i}{ks}\frac{\partial f_o}{\partial \eta_o}\frac{dA(y)}{dy} \quad . \tag{A.12}$$

The integrability condition on the second order equation (A.9) is

$$\left\{\frac{1}{2}\left\langle f_o \frac{\partial^2 \mathcal{L}_o}{\partial \eta_o^2} f_o \right\rangle + \left\langle f_o \frac{\partial \mathcal{L}_o}{\partial \eta_o}\frac{\partial f_o}{\partial \eta_o}\right\rangle\right\}\frac{d^2A}{dy^2} - (\omega - \omega_o(x))\left\langle f_o \frac{\partial \mathcal{L}_o}{\partial \omega_o} f_o\right\rangle A(y) = 0, \tag{A.13}$$

and using the relation

$$\frac{1}{2}\left\langle f_o \frac{\partial^2 \mathcal{L}_o}{\partial \eta_o^2} f_o \right\rangle + \left\langle f_o \frac{\partial \mathcal{L}_o}{\partial \eta_o} \frac{\partial f_o}{\partial \eta_o} \right\rangle + \frac{1}{2}\frac{\partial^2 \omega_o}{\partial \eta_o^2}\left\langle f_o \frac{\partial \mathcal{L}_o}{\partial \omega_o} f_o \right\rangle = 0 \qquad (A.14)$$

this can be reduced to

$$\frac{1}{2}\frac{\partial^2 \omega_o}{\partial \eta_o^2}\frac{d^2 A}{dx^2} + k^2 s^2(\omega - \omega_o(x))\, A(x) = 0 \qquad (A.15)$$

where we have now set $h = 1$ and discarded the scaled coordinate y in favour of x throughout.

Eq. (A.15), which is the central result of the higher order theory, completes the determination of ω and of the mode structure. This equation depends only on $\omega_o(x)$ and is similar in form to that for a plane slab (and might therefore be referred to as the equivalent plane slab problem) but the toroidal effects are incorporated through the function $\omega_o(x)$.

When $\omega_o(x)$ is fully complex there are well localised solutions of (A.15), but if $\omega_o(x)$ is almost real (weak damping) well localised solutions exist only if

$$\frac{\partial^2 \omega_o}{\partial \eta_o^2} \cdot \frac{\partial^2 \omega_o}{\partial x^2} > 0 \, . \qquad (A.16)$$

If $\omega_o(x)$ is real but (A.16) is not satisfied then the solutions of (A.15) are oscillatory and may extend over a wide region. In this event the boundary conditions to be applied to (A.15) depend upon what additional physical processes come into play at the boundary.

At this point we must return to the question of whether it is legitimate to treat $(\omega - \omega_o(x))$ as a small quantity, formally of order $h^{2\nu}$, as is necessary if (A.15) is to be self-consistent. There are two important situations where this is strictly correct. In the first we expand $\omega_o(x)$ about a stationary point, $\omega_o(x) = \hat{\omega} + \omega_o''(x).x^2/2$, making

(A15)

$$\frac{1}{2}\frac{\partial^2\omega_o}{\partial\eta_o^2}\frac{d^2A}{dx^2} + k^2s^2\left((\omega - \hat{\omega}) - \frac{\partial^2\omega_o}{\partial x^2}\cdot\frac{x^2}{2}\right)A = 0 \qquad (A17)$$

Solutions of this equation have a width $\Delta r/r \sim (kr_n)^{-\frac{1}{2}}$ and $(\omega - \omega_o(x))$ is $\sim (kr_n)^{-1}$ so that (A17) is entirely self consistent and corresponds to $\nu = \frac{1}{2}$.

In the second case we expand $\omega_o(x)$ about a W.K.B. turning point, making (A15)

$$\frac{1}{2}\frac{\partial^2\omega_o}{\partial\eta_o^2}\frac{d^2A}{dx^2} - k^2s^2\left(\frac{\partial\omega_o}{\partial x}\right).xA(x) = 0 \qquad (A18)$$

This is again self consistent and corresponds to $\nu = 1/3$.

More generally, a W.K.B. solution of (A15) leads to the phase integral condition

$$\oint(\omega - \omega_o(x))^{\frac{1}{2}}dx = \oint \kappa\, dx = \frac{(2m + 1)\pi}{ks}\left(\frac{1}{2}\frac{\partial^2\omega}{\partial\eta_o^2}\right)^{\frac{1}{2}} \qquad (A19)$$

and this is consistent with $(\omega - \omega_o(x))$ small so long as $m \ll kr$. However in this event it would, formally, be equally valid to expand $\omega_o(x)$ and to use Eq. (A17). To obtain solutions corresponding to larger values of m the W.K.B. ansatz should be made at an earlier stage[1], by setting $A \sim \exp i\int\kappa\,dx$. Then the lowest order equation defines κ by

---

[1]This approach has been used by Frieman, Dewar, Glasser, and others [12] and by Lee and Van Dam and others [13] and more recently, specifically for drift waves, by Frieman [14]. These authors have established (A19) as the correct W.K.B. connection formula. We are grateful to them for various discussions and for informing us of their results.

$$\omega_o(\kappa, x) = \omega . \qquad (A20)$$

Eq. (A18) is still required in the vicinity of the turning points where $\kappa \sim 0$ and ω is determined from the W.K.B. integral as in (A19).

Summary

The higher order theory always produces a second eigenvalue equation, this time in the (radial) x-coordinate. In effect, therefore, our formalism replaces the original two-dimensional problem by two one-dimensional problems. The first problem is in the η-coordinate, with an effective potential $U(\eta)$, and yields $\omega_o(x,\eta_o)$ and the shape of the perturbation in η. The second problem is in the x-coordinate and uses $\omega_o(x,\eta_o)$ as an effective potential to determine ω and the shape of the perturbation in x - so completing the solution. Thus the entire solution is contained within the function $\omega_o(\eta_o,x)$ which we computed in the main text. In this description the effects of toroidal modulation first enter (and are easily visualised) through the modulation of the effective potential $U(\eta)$. The effects are thereby incorporated in $\omega_o(\eta_o, x)$ which in turn incorporates them in the final (equivalent plane slab) eigenvalue problem.

There is, however, one reservation to be made. The development of the higher order theory uses a formal expansion in a parameter which can be expressed as $(a_i/r)(ka_i)^{-1}$. However the basic 2-D model, Eq. (4) is itself an approximation based on an expansion in a_i/r and r/R and is correct only to zero order. Consequently adoption of an improved basic 2-D model, which retained terms of order (a_i/r) would affect Eq. (A.15). However the general structure of the higher order theory described above is applicable to any 2-D model.

REFERENCES

[1] PEARLSTEIN, L.D., BERK, H.L., Phys. Rev. Letts. 23 (1969) 220.

[2] ROSS, D.W., MAHAJAN, S.M., Phys. Rev. Letts. 40 (1978) 324.

[3] TSANG, K.T., CATTO, P.J., WHITSON, J.C., SMITH, J., Phys. Rev. Letts. 40 (1978) 327.

[4] TAYLOR, J.B., Proceedings 6th International Conference on Plasma Physics and Controlled Thermonuclear Research, Berchtesgaden, Oct. 1976.

[5] CORDEY, J.G., HASTIE, R.J., Nucl. Fusion 17 (1977) 523.

[6] CONNOR, J.W., HASTIE, R.J., TAYLOR, J.B., Phys. Rev. Letts. 40 (1978) 396.

[7] CONNOR, J.W., HASTIE, R.J., TAYLOR, J.B., Proc. Roy. Soc., 365 (1979) 1.

[8] HORTON, Jr., W., ESTES, R., KWAK, H., DUK-IN CHOI, Phys. Fluids 21 (1978) 1367.

[9] HAMMING, R.W., Numerical Methods for Scientists and Engineers (McGraw-Hill, New York, 1962), p.215.

[10] HUGILL, J., private communication.

[11] CONNOR, J.W., HASTIE, R.J. and TAYLOR, J.B., Proceedings 7th International Conference on Plasma Physics and Controlled Thermonuclear Research, Innsbruck, 1978.

[12] CHANCE, M.S., et. al., Proceedings of 7th International Conference on Plasma Physics and Controlled Thermonuclear Research, Innsbruck, 1978.

[13] LEE, Y-C, et. al., Proceedings of 7th International Conference on Plasma Physics and Controlled Thermonuclear Research, Innsbruck, 1978.

[14] FRIEMAN, E.A. Private Communication.

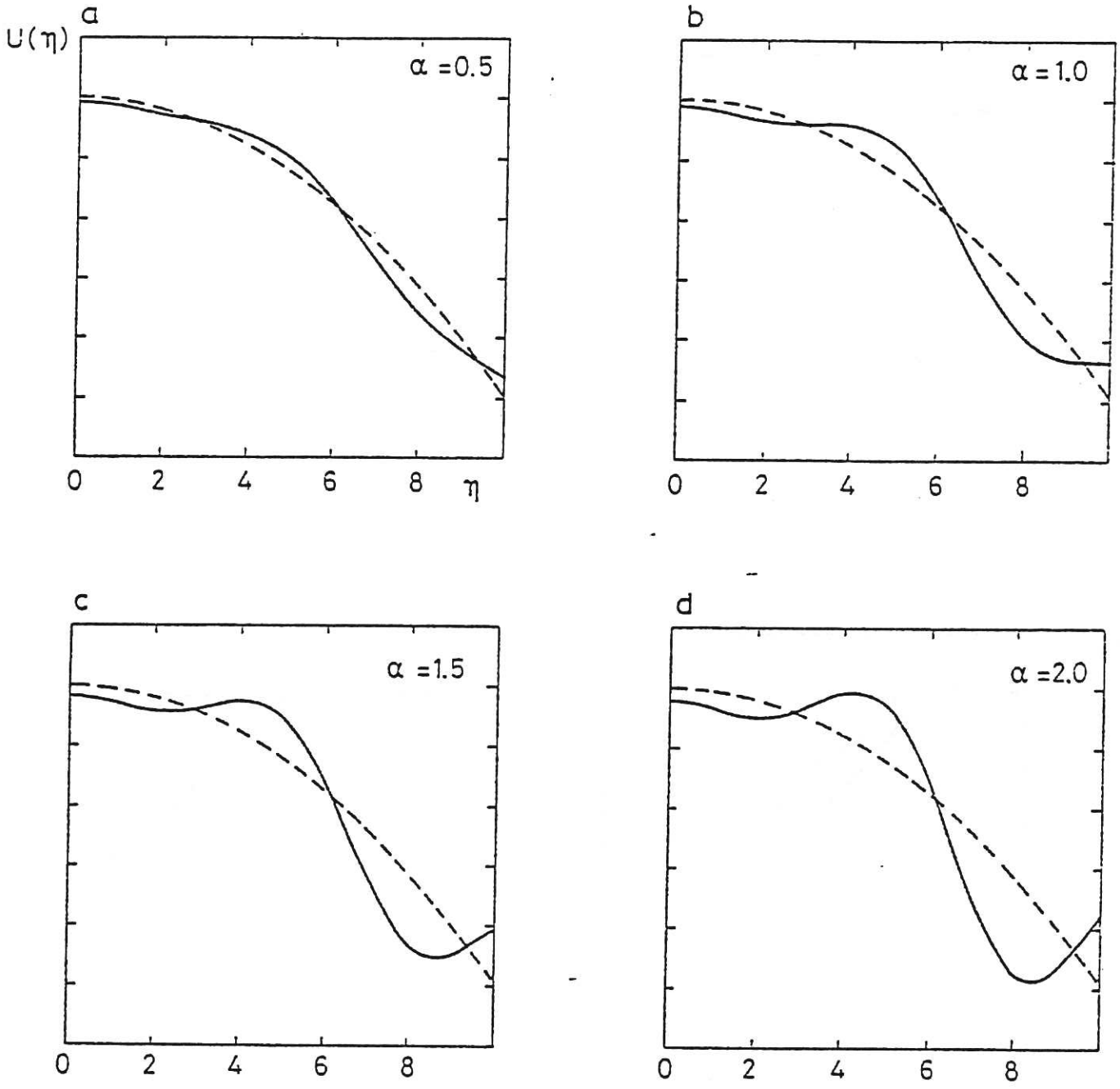

Fig.1 The potential $U(\alpha, \eta)$ for s = 1 and $\eta_0 = 0$. (1a) $\alpha = 0{\cdot}5$; (1b) $\alpha = 1{\cdot}0$; (1c) $\alpha = 1{\cdot}5$; (1d) $\alpha = 2{\cdot}0$. The broken line is $U(\alpha \equiv 0, \eta)$.

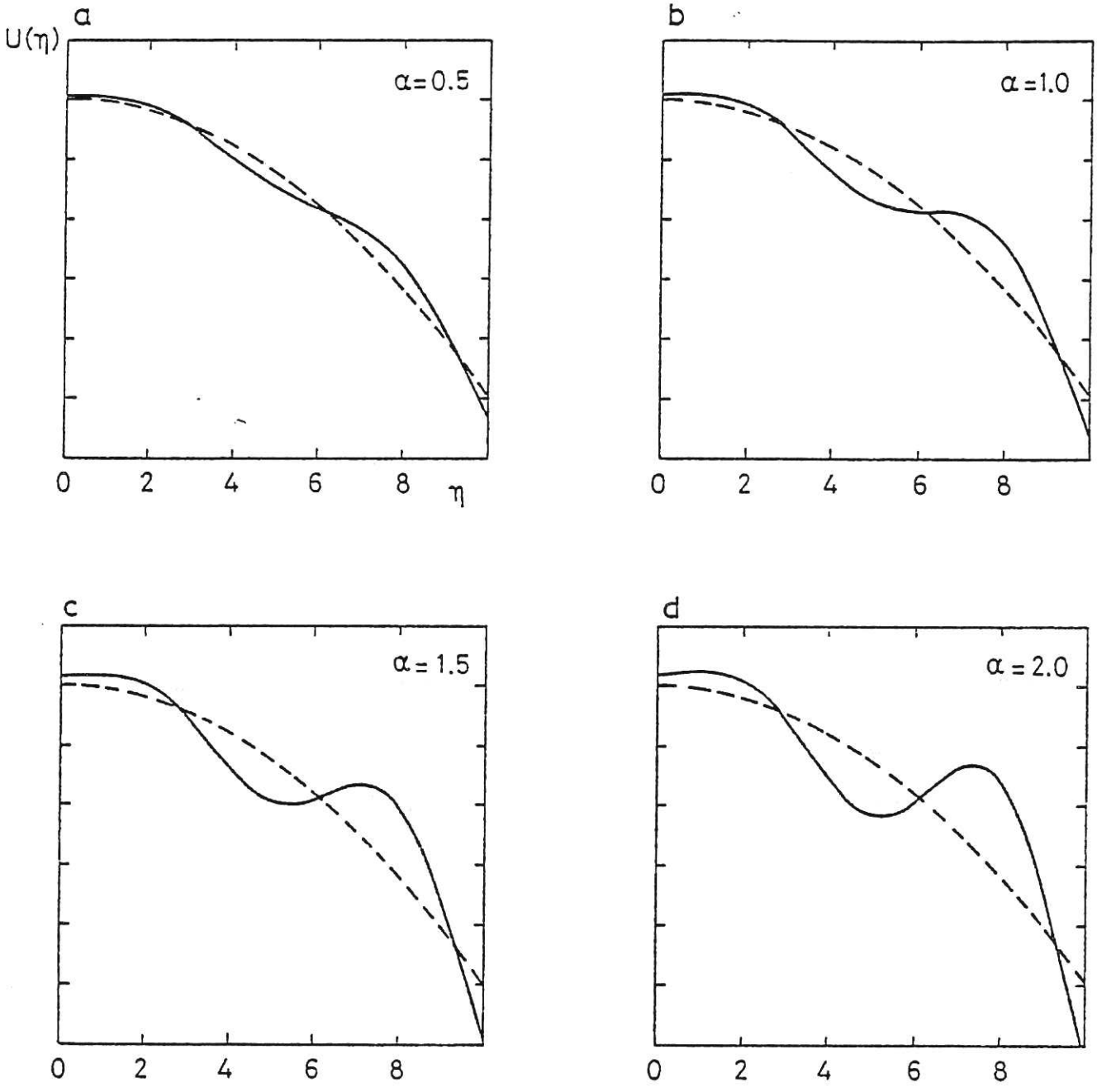

Fig.2 The potential $U(\alpha,\eta)$ for $s = 1$ and $\eta_0 = \pi$. (2a) $\alpha = 0{\cdot}5$; (2b) $\alpha = 1{\cdot}0$; (2c) $\alpha = 1{\cdot}5$; (2d) $\alpha = 2{\cdot}0$.

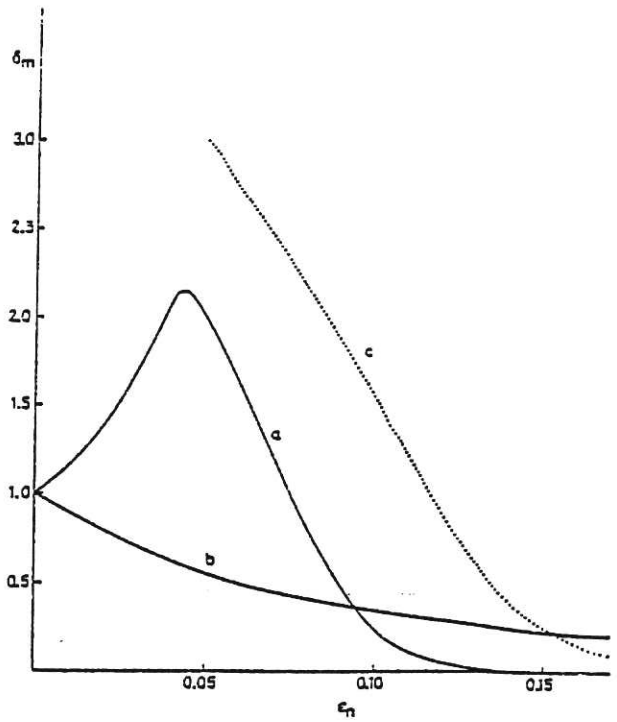

Fig.3 The shear damping as measured by δ_m (the electron driving required for a marginally stable mode) as a function of the modulation parameter ϵ_n. Curve 3a, for $\eta_o = 0$ i.e. modes centred on the outside of the minor cross section. Curve 3b, for $\eta_o = \pi$, i.e. modes centred on the inside. Curve 3c, for $\eta_o = 0$, a higher harmonic solution. In Fig.3, the other parameters have the values $k^2 a_i^2 = 0{\cdot}1$, $\epsilon_c = 0{\cdot}1$, $s = 1$, and δ_m has been normalised to unity at $\epsilon_n = 0$.

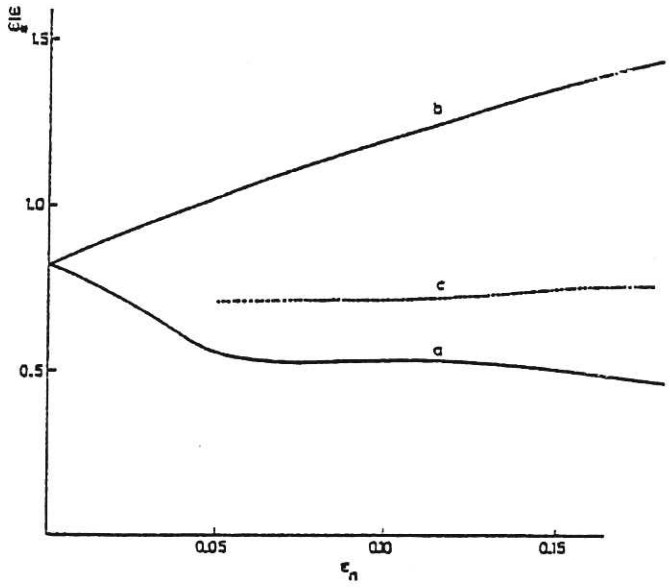

Fig.4 The frequency ω normalised to ω_* as a function of ϵ_n. Curve 4a for $\eta_o = 0$, curve 4b for $\eta_o = \pi$, curve 4c for $\eta_o = 0$ higher harmonic. All parameters as in Fig.3.

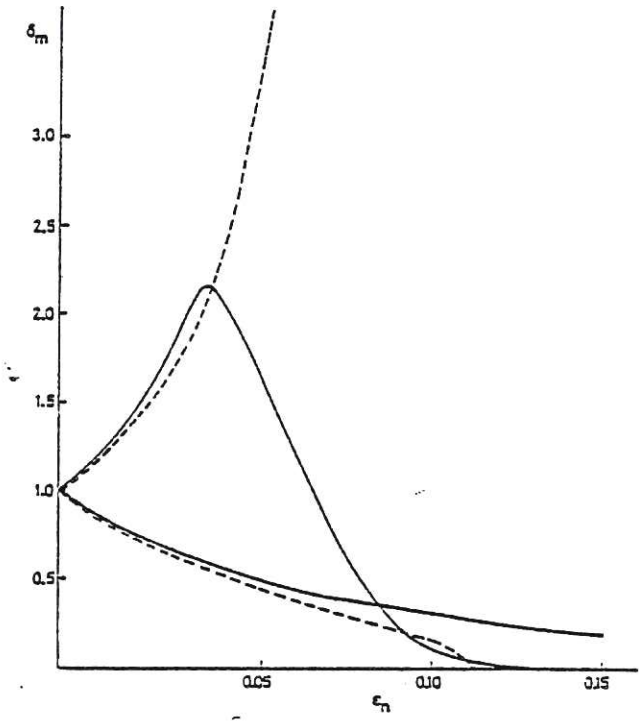

Fig.5 Comparison of δ_m as shown in Fig.3a,b (solid curves) with the analytic result given by the strong coupling theory for δ_m (dashed curves).

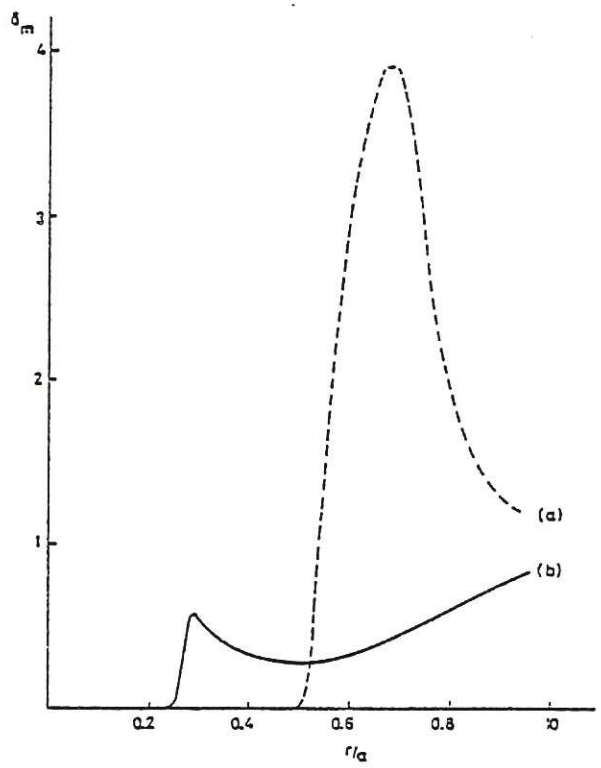

Fig.6 The shear damping as measured by δ_m (normalised to $\delta_m(\epsilon_n \equiv 0)$) as a function of r/a for typical q and n profiles in DITE tokamak. $q = (1 + 4\,r^2/a^2)$, $n \sim n_0(1 - r/a)$ and aspect ratio a/R = 1/5. Curve 6a for $\eta_0 = 0$; 6b for $\eta_0 = \pi$.

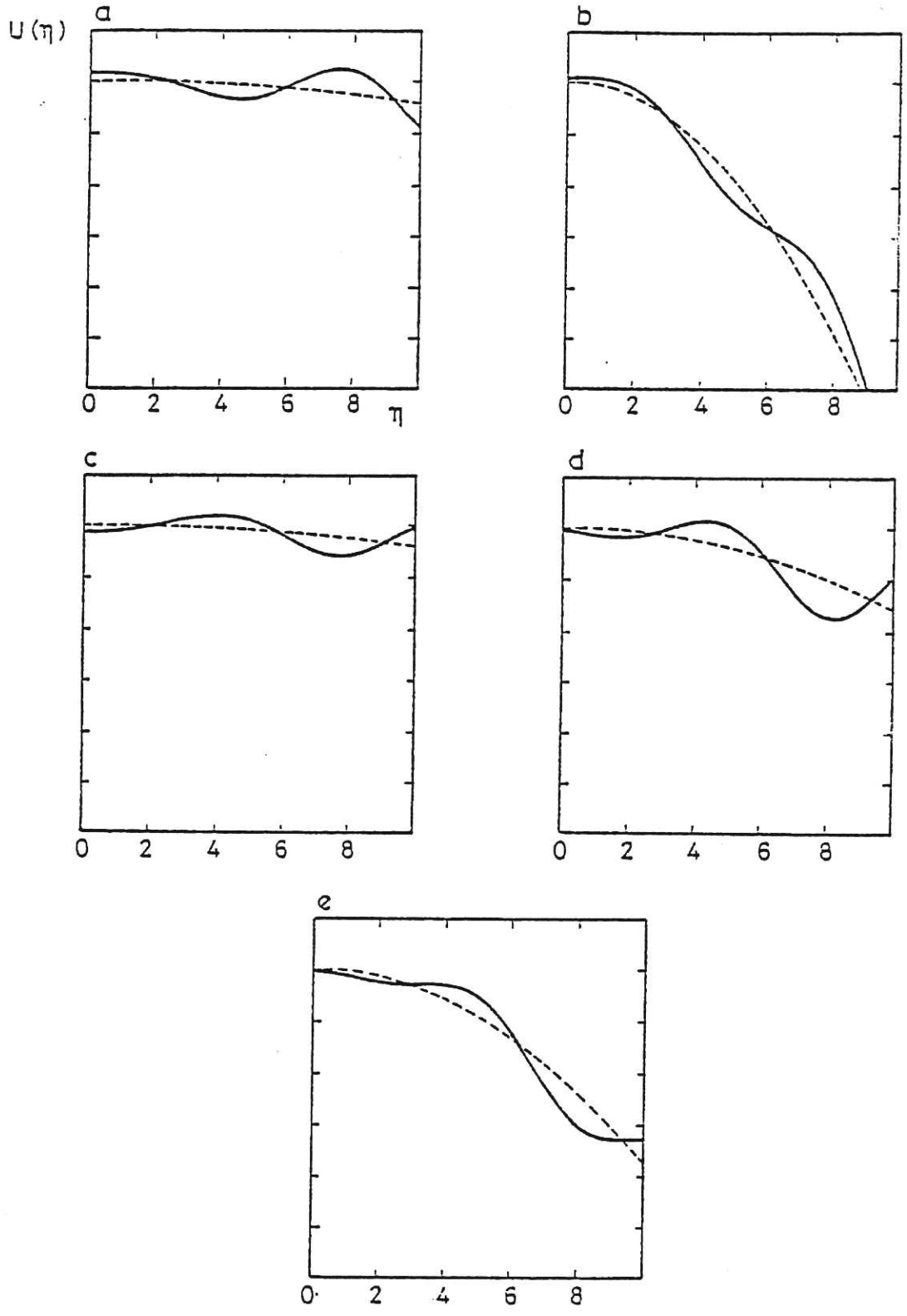

Fig.7 The structure of $U(\eta)$ for $\eta_o = 0$ and π at various radii in the DITE tokamak with profiles taken as $q \sim 1 + 4r^2/a^2$, $n \sim n_o(1 - r/a)$. The broken line shows the potential U for the equivalent slab problem ($\epsilon_n \equiv 0$). The parameters appropriate to each case are:- $k^2 a_i^2 = 0{\cdot}1$ and, (a) $\eta_o = \pi$, $r/a = 0{\cdot}25$; (b) $\eta_o = \pi$, $r/a = 0{\cdot}6$; (c) $\eta_o = 0$, $r/a = 0{\cdot}2$; (d) $\eta_o = 0$ $r/a = 0{\cdot}4$; (e) $\eta_o = 0$, $r/a = 0{\cdot}7$.